Rare Metal Materials and Engineering
Volume 48, Issue 11, November 2019
Available online at www.rmme.ac.cn

Science Press

Cite this article as: Rare Metal Materials and Engineering, 2019, 48(11): 3463-3469.

ARTICLE

Effect of Hot Deformation on the Mechanical Properties of Electron Beam Welded TC11/Ti_2AlNb Alloys

Qin Chun[1,2], Yao Zekun[2]

[1] *North Minzu University, Yinchuan 750021, China;* [2] *Northwestern Polytechnical University, Xi'an 710072, China*

Abstract: Nanoindentation and Vikers indentation tests were carried out to characterize the hardness and elastic modulus profiles in the vicinity of welding area for TC11/Ti_2AlNb alloys in different conditions. Distribution of nano/micro scale mechanical behavior was analyzed in combination with the microstructure. The results show that the decomposed martensite α' phase is the major contributor to the reduction in hardness of the heat affected zone of TC11 alloy. Phases precipitated in welding zone and heat affected zone of Ti_2AlNb alloy result in an increase of the hardness. Forging and heat treatment processes can improve the elastic modulus of the welding area. After welding, the elastic modulus is only ~92 GPa in the welding zone, but the value increases to ~130 GPa after heat treatment. Meanwhile, the yield strength of the welding zone increases after deformation treatment, which is consistent with the variation of hardness and elastic modulus in the welding area.

Key words: nanoindentation; titanium alloy; intermetallics; mechanical properties; microstructure

Titanium alloy TC11 and Ti_2AlNb-based intermetallics are widely used in aerospace for their attractive properties such as strength, weight ratio and creep resistance[1, 2]. Electron beam welding (EBW) is a fusion welding process with high density of energy in a vacuum environment, which can be used to join refractory metals and dissimilar alloys without filler metals[3]. After EBW process, the microstructures of weld are solidified crystals with coarse columnar grains and equiaxed grains. Hot processing can improve the microstructure of the weld and enhance the weld performance[4]. For the joining of Ti-Al-Nb alloy to titanium alloy using EBW technique, some works have shown that the tensile strength of dissimilar alloys joint is well[5-7]. The mechanical properties in the bore and rim of compressor disc are different. If the Ti_3Al base ordered intermetallic alloy is joined with TC11 alloy, the combination disc can meet different performance requirements[6].

Oliver-Pharr analysis for nanoindentation has been proven an effective and convenient method of determining the elastic modulus (E) and hardness (H) of solids[8]. It has been rapidly developed and widely used to identify the phases clearly and to characterize the mechanical properties of materials in micro or even nano scale[9, 10]. Additionally, some works have been done to analyze the hardness variation of welding interfaces using nanoindentation[11-16]. Lee[17] found through nanoindentation test that the hardening effects are caused by the precipitation of the γ' phase in Ni_3Al-based alloy. During the welding process, elemental diffusion causes the microstructure of the fusion zone to be different from that of the base metals. It is difficult to quantitatively characterize the interface using a conventional experimental technique. To date, the researches on welding dissimilar titanium alloys using EBW are mainly focused on the microstructure and tensile strength[5-7]. There are few reports on the mechanical properties of welding interface using nanoindentation.

In the present study, TC11 alloy and Ti_2AlNb-based intermetallics were joined by EBW process, followed by forging and heat treatment. The main aim of this work is to show how much mechanical properties are influenced by nanoindentation technique in different conditions.

Received date: November 19, 2018
Foundation item: National Natural Science Foundation of China (51804011)
Corresponding author: Qin Chun, Candidate for Ph. D., School of Materials Science and Engineering, North Minzu University, Yinchuan 750021, P. R. China, Tel: 0086-951-20667378, E-mail: qinchun0131@163.com

1 Experiment

Two alloys were both forged to required dimensions and spark machined to cuboid specimens (20 mm×25 mm×35 mm for EBW and 20 mm×25 mm surface for welding). The microstructures of base metals for welding are illustrated in Fig.1. The parent TC11 alloy presents a typical bimodal microstructure consisting of an equiaxed α with an average grain size of 5 um and transformed β with a secondary lamellar α thickness of 0.6 μm (Fig.1a). The microstructure of Ti_2AlNb alloy is composed of α_2+O+B2 phases, in which α_2 phase is distributed in the grain boundary and fine O phase is precipitated in the B2 matrix (Fig.1b).

The welded surfaces were polished and cleaned before welding. Welding experiments were conducted using a KS55-G150 model EBW machine. The welding parameters are listed in Table 1. After welding, nearly isothermal deformation was carried out on THP-630A model hydraulic machine which allows the specimens to be pressed at a constant strain rate. During the deformation process, the temperature of dies was kept at 950 °C. The specimens were heated to the appointed temperature 980 °C and held in the box heat treatment furnace for 18 min. The deformation direction was parallel to the welding interface. After forging, the specimen was air cooled (AC). Subsequently, heat treatment of specimens with 960 °C/1 h, AC + 600 °C /4 h and AC was carried out in the heat treatment furnace. HV indentation was performed using an indenter load of 0.98 N with 15 s loading time, and the indentations were spaced 250 um apart. Nanoindentation testing

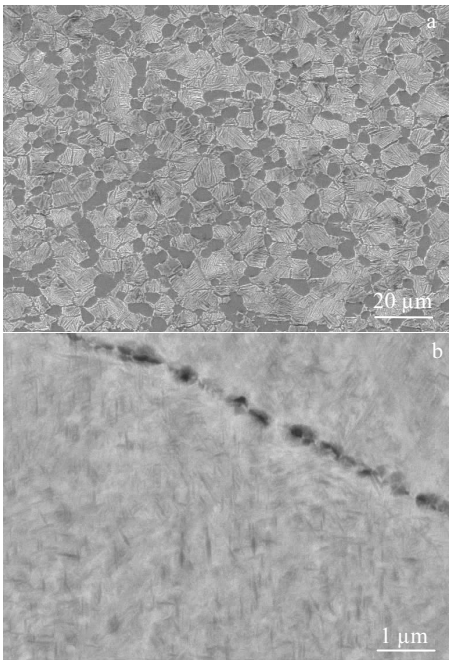

Fig.1 Microstructures of base metals for EBW process: (a) TC11 alloy and (b) Ti_2AlNb alloy

Table 1 Welding parameters of TC11/Ti_2AlNb dual-alloy

Parameter	Accelerate voltage/kV	Focusing current/mA	Welding current/mA	Welding speed/ mm·s^{-1}
Seal welding	150	2250	8	8
Welding (one side)	150	2250	14	8
Welding (other side)	150	2250	10	8

was conducted by a Triboscope nanomechanical testing system (Hysitron, Minneapolis, MN) equipped with a scanning probe microscope for imaging. The modulus and hardness values were calculated based on the indentation load-displacement data via the Oliver-Pharr method[8]. The applied load was 300 mN with 50 s loading and unloading segment time and 5 s of holding time.

2 Results

2.1 Materials

The microstructures of welding zone in different conditions are shown in Fig.2. Fig.2a and 2b show the microstructures of TC11/Ti_2AlNb alloy weldment under welding condition. The near HAZ of TC11 alloy is mainly composed of martensite α' phase that is arranged in a random direction. The β grains are strongly coarsened during the welding process (Fig.2a). Fig.2b shows that the HAZ of Ti_2AlNb alloy consists of a single β phase due to the high Nb content of Ti_2AlNb alloy, and the grain boundaries extend to the welding zone. The welding zone is also composed of β grains.

After nearly isothermal forging, the microstructures of welding area change greatly (Fig.2c, 2d). It should be noted that the deformation temperature (980 °C) is within (α+β) two phase region and (α_2+O+B2) three-phase region for TC11 alloy and Ti_2AlNb alloy, respectively. Many α laths appear in the HAZ of TC11 alloy with the content of about 70% (Fig.2c). This is because the martensite α' phase is mainly transformed into α laths and residual β phase during the high temperature heating process before deformation. During the deformation process, these α laths are deformed along the metal flowing direction, resulting in the morphology of the microstructure above. After deformation, the grain boundaries in Ti_2AlNb HAZ are composed of α_2 phase and expand to the fusion zone (Fig.2d). As the deformation temperature is high, the fusion zone has a few phases precipitated with the recrystallization of β grains.

The microstructures of TC11/Ti_2AlNb alloy weldments after heat treatment are shown in Fig 2e and 2f. It can be seen that the microstructure of HAZ of TC11 alloy consists of primary α and transformed β. α laths and residual β phase obtained from the deformation process are transformed during the heat treatment. The secondary α phases precipitate from the residual β phase, resulting in the transformed β microstructure. At the interface front of HAZ of TC11 alloy, the mi-

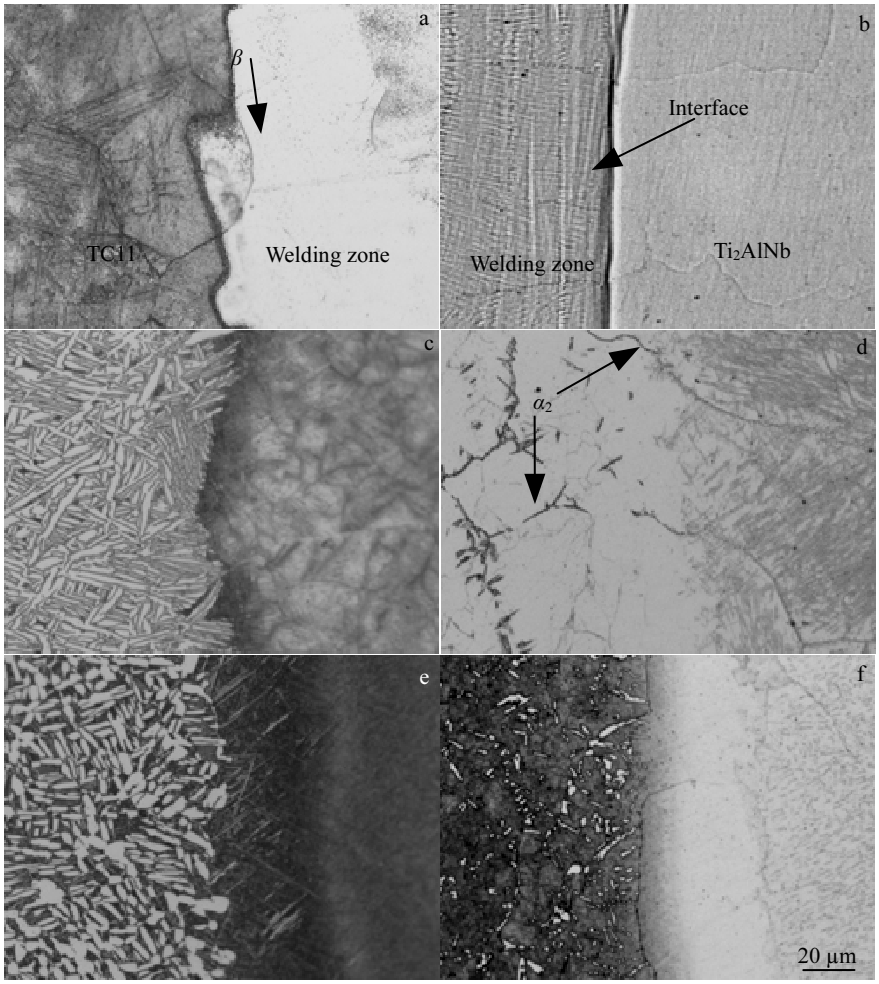

Fig.2 Microstructures of welding zone in different conditions: (a, b) welding, (c, d) forging, and (e, f) heat treatment

crostructure consists of acicular α which precipitates and grows during the heat treatment. The microstructure of welding zone near HAZ of Ti_2AlNb alloy changes significantly after heat treatment and more α_2 phases precipitate, which is different from the microstructure of welding zone near HAZ of TC11 alloy (Fig.2f). This is because the Al content in this area is high, which benefits the precipitated α_2 phases.

2.2 Microhardness investigation

Fig.3 shows the Vickers microhardness ($HV_{0.1}$) profile obtained across the HAZ of the welding zone. The hardness varies obviously in different conditions. These results are related to the microstructures obtained by different processes. The hardness of HAZ of TC11 alloy in welding condition is higher than in other conditions. During welding, the HAZ of TC11 alloy consists of hard phase martensite α' because the temperature of the welding zone exceeds the β phase transformation point of base metal. The hardness of the welding zone and HAZ of Ti_2AlNb is lower, 2.95 and 3.15 GPa, respectively, because these areas are mainly composed of soft β phase. After forging, the hardness of HAZ of TC11 alloy drops while

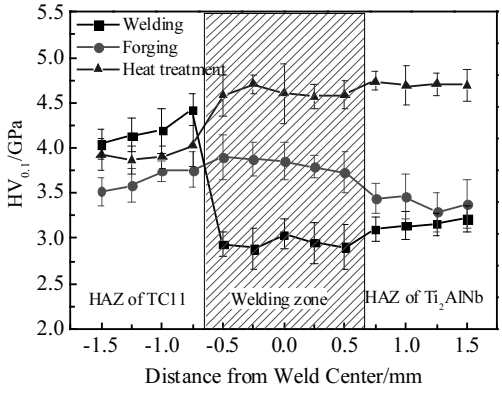

Fig.3 Vickers microhardness indentation profile across the weld

hardness of other areas increases. This is because the HAZ of TC11 alloy consists of α phase after forging whose hardness is lower than that of α' phase. While α_2 phase at grain boundary and a little α_2 phase in grains are precipitated in welding zone and HAZ of Ti_2AlNb alloy, resulting in an increase in the hardness. Compared with forging condition, hardness in-

creases in all areas after heat treatment condition. Hardness in HAZ of TC11 alloy reaches 3.93 GPa, while it reaches 4.61 and 4.71 GPa in welding zone and HAZ of Ti_2AlNb alloy, respectively. Combined with the microstructures mentioned above, it is suggested that precipitation hardening is one of the reasons for determining the hardness.

2.3 Nanohardness investigation

For microhardness and nanohardness investigations, uniform specimens were used. However, it should be mentioned that exactly the same area cannot be investigated, but similar properties in adjusted regions of the microstructure were assumed. Typical load progression (load-displacement or *P-h*) curves during nanoindentation for HAZ of TC11 alloy and welding zone under heat treatment condition are shown in Fig.4a. Micrograph of Berkovich impression for HAZ and welding zone is shown in Fig.4b. Based on the half-space elastic deformation theory, hardness (H) and elastic modulus (E) values can be extracted from the experimental data (load-displacement curves) using the O&P method [8]. Conventional nanoindentation hardness refers to the mean contact pressure; this hardness, which is the contact hardness (H_c), can be calculated based on Eq.(1~3)[8].

$$H_c = \frac{P_{max}}{A_c} \quad (1)$$

where

$$A_c = 24.5h_c^2 + C_1h_c + C_2h_c^{1/2} + ... + C_8h_c^{1/128} \quad (2)$$

and

$$h_c = h_{max} - \varepsilon\frac{P_{max}}{S} \quad (3)$$

where A_c is projected contact area between the tip and the substrate at peak load, h_{max} is total penetration depth of the indenter at peak load, P_{max} is peak load at the indenter displacement depth h_{max}, and ε is an indenter geometry constant equal to 0.75 for Berkovich indenter. S is unloading stiffness defined as the initial slope of the unloading load-displacement curve at the maximum depth of penetration. The expressions for calculating the elastic modulus from indentation experiments are based on Sneddon's elastic contact theory [18]:

$$E_r = \frac{S\sqrt{\pi}}{2\beta\sqrt{A_c}} \quad (4)$$

where β is a constant that depends on the geometry of the indenter (β=1.167 for Berkovich tip)[12].

It is assumed that the surface effects on the nanohardness can be minimized since the specimens were chemically etched and indentation depth was about micron scales. Referring to the *P-h* curves of HAZ of TC11 alloy and welding zone in Fig.4a, the slope of the curves increases due to increase in contact area during indentation. The maximal indenter displacement (h_{max}) at a peak load of 300 mN for HAZ of TC11 alloy is 1747 nm, larger than 1604 nm of welding zone, and the final displacement after complete unloading (h_f) is 1432 and 1229 nm, respectively. The elastic modulus for welding zone is 129.26 GPa, while it can reach 143.26 GPa in HAZ of TC11 alloy. However, the nanohardness of HAZ of TC11 alloy (4.71 GPa) is lower than that of the welding zone (5.96 GPa).

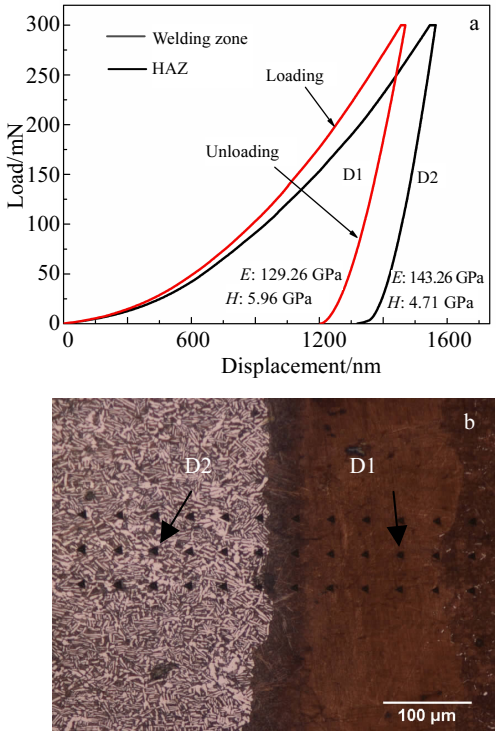

Fig.4 Load-displacement curves of TC11 alloy (a) and image of Berkovich impression with marked indentation lines (b) (D1: welding zone, D2: HAZ)

Elastic modulus and nanohardness (H_{nano}) profiles of welding interface in different conditions are shown in Fig.5. Nanoindentation tests were performed to characterize the mechanical property in the vicinity of the weld area. In the same condition, the elastic modulus and nanohardness in different areas within the welding zone have few differences. The E profiles in the welding areas present a "U" shape, indicating that the E of welding zone is lower than that of the base metals. After welding, E in welding zone is only ~92 GPa, which is because the microstructure of welding zone is composed of β phase. The constituent phases of titanium alloys have different elastic modulus values. The β phase exhibits a significantly lower elastic modulus than α phase [19, 20]. Moreover, Kim et al[21] have reported that metastable β phase has a lower elastic modulus than stable β phase. In different conditions, the E of welding zone changes greatly. In association with the microstructures, during forging process, metastable β obtained from the welding process is transformed into stable phase and a few α_2 phases precipitate along the grain boundaries.

During heat treatment process, the microstructure of welding zone near TC11 alloy was composed of acicular α phase, which was composed of α_2 phase near the Ti_2AlNb alloy. Change in microstructures results in an increase of the E. It can be observed that E of the two areas after heat treatment is at the same level for ~130 GPa, increased by 41% compared with that after welding condition. In welding condition, the E of HAZ of TC11 alloy and Ti_2AlNb alloy is ~135 and ~127 GPa, respectively, and after heat treatment process, E of the two areas increases to ~149 and ~148 GPa, respectively. These changes are principally concerned with the microstructures of α phase (HAZ of TC11 alloy) and α_2 phases (HAZ of Ti_2AlNb alloy) precipitated. Meanwhile, the solution strengthening during heat treatment process also has a positive effect on the E value. Tang et al[22] have reported that E of Ti_2AlNb-based alloy with B2 and B2+O phases is ~100 and ~120 GPa, respectively, similar to the present results.

From Fig.5, it can be seen that nanohardness has the same change trends with Vickers microhardness. For the welding condition, the nanohardness is ~4.59 GPa in the HAZ of TC11 alloy, ~3.73 GPa in the welding zone, and ~4.31 GPa in HAZ of Ti_2AlNb alloy. In the HAZ of TC11 alloy side, the nanohardness descends as the α' phase is decomposed during forging or heat treatment process. After heat treatment process, the nanohardness of welding zone reaches ~5.98 GPa, increased by 60% compared with that in the welding condition. It suggests that the hardness and elastic modulus of welding zone can be increased through forging and heat treatment. Similar to the HV, the max nanohardness appears in the HAZ of Ti_2AlNb alloy after heat treatment which reaches ~6.28 GPa.

It can be found that transverse distribution of HV and H_{nano} presents the similar shape and the values of base metals and welding zone decrease in parallel. But the values of nanohardness are higher than that of Vickers hardness. This is largely due to the indentation size effect[17, 23]. In comparison, the Vickers hardness is a macroscopic measurement that is the average value of grain boundary, precipitation, base matrix, etc. The nanoindentation is used to characterize the microhardness, elastic modulus of materials in micrometers and even several hundreds of nanometers. So the nanoindentation can be used in smaller areas. The experimental results show that the HV test results can be reliably compared with the H_{nano} obtained from the nano-mechanical test with a Berkovich indentation. So the H_{nano} and HV tests can be used complementarily to analyze the hardness distribution of electron beam welded alloys.

2.4 Mechanical properties at room temperature

The tensile properties of the weldments in different conditions at room temperature are given in Table 2. It can be noted that the tensile yield strength increases after forging+heat treatment. In welding condition, the yield strength (YS) is only 920 MPa, while after deformation treatment, the yield strength increases to 1140 MPa. The tensile fractographs of dual-alloy weldments are shown in Fig.6. The weldment after welding shows the intergranular fracture as the welding zone consists mainly of β grains (Fig.6a). In Fig.6b, the fracture morphology shows a predominantly transgranular fracture over the fracture surface with shallow dimples and torn edges. In the welding condition, fracture accompanied with necking occurs in the HAZ of Ti_2AlNb and welding zone. This is because the microstructure of HAZ of Ti_2AlNb predominantly contains β phase which has a better plasticity and a low strength. The tensile deformation easily occurs in this area. After deformation treatment, phases precipitated in HAZ of Ti_2AlNb and weld will affect the mechanical properties, resulting in an increase in the yield strength and difficulty in tensile deformation. It can be seen that phases precipitated can improve the yield strength and reduce the elongation. Compared with Fig.5, the sharp increase in hardness and elastic modulus after deformation treatment is consistent with the results of the tensile test, in which an increase of the yield strength was observed.

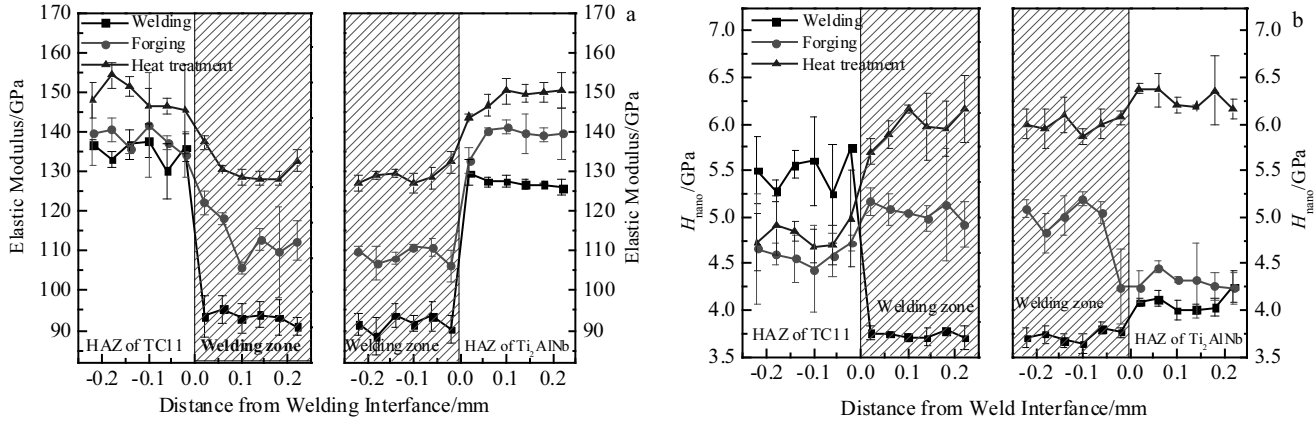

Fig.5 Elastic modulus (a) and nanohardness H_{nano}(b) of welding interface in different conditions

Table 2 Mechanical properties of weldments in different conditions at room temperature

Condition	UTS/ MPa	YS/ MPa	Elongation/%	Fracture area
Welding	935	920	6.5	Weld
Deformation	1190	1140	3.2	Weld

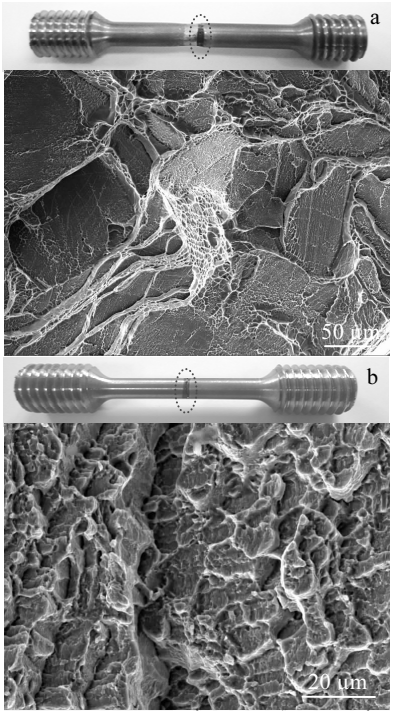

Fig.6 Tensile fractographs of dual-alloy weldments in different conditions tested at room temperature: (a) welding and (b) deformation treatment

3 Conclusions

1) The decomposed martensite α' is the major contributor to the reduction of hardness in HAZ of TC11 alloy. Phases precipitated in welding zone and HAZ of Ti_2AlNb alloy result in an increase in the hardness.

2) The elastic modulus profile of welding area presents a "U" shape. Forging or heat treatment can improve the elastic modulus. After welding, the elastic modulus is only ~92 GPa in welding zone, but it increases to ~110 and ~130 GPa after forging and heat treatment, respectively.

3) The transverse distribution of HV and H_{nano} presents the similar shape and the values of base metals and welding zone decrease in parallel. The measured values of nanohardness are higher than that of the Vickers microhardness,

4) After deformation treatment, the yield strength of welding zone increases, consistent with the results from the nanoindentation test, in which an increase of hardness and elastic modulus in welding zone is obtained.

References

1 Gu Yi, Qi Yanling, Xia Changqing *et al*. *The Chinese Journal of Nonferrous Metals*[J], 2013, 23(4): 997
2 Wu Hongyan, Zhang Pingze, Chen Wei *et al*. *The Chinese Journal of Nonferrous Metals*[J], 2009, 19(5): 1121
3 Wang Shaogang, Wu Xingqiang. *Materials and Design*[J], 2012, 36: 663
4 Tan Lijun, Yao Zekun, Qin Chun *et al*. *The Chinese Journal of Nonferrous Metals*[J], 2010, 20(8): 1533
5 Zhang Hongtao, He Peng, Feng Jicai *et al*. *Materials Science and Engineering A*[J], 2006, 425(1): 255
6 Tan Lijun, Yao Zekun, Zhou Wei *et al*. *Aerospace Science and Technology*[J], 2010, 14 (5): 302
7 Tan Lijun, Yao Zekun, Ning Yongquan *et al*. *Materials Science and Technology*[J], 2011, 27(9): 1469
8 Olivier W C, Pharr G M. *Journal of Materials Research*[J], 1992, 7(6): 1564
9 Liao Chengwei, Chen Jianchun, Li Yang *et al*. *Journal of Materials Science and Technology*[J], 2012, 28(6): 524
10 Li Yang, He Kang, Liao Chengwei *et al*. *Journal of Materials Research*[J], 2012, 27(1): 192
11 Huang Y M, Li Y, He K *et al*. *Materials Science and Technology*[J], 2011, 27(9): 1453
12 Koumoulos E P, Charitidis C A, Daniolos N M *et al*. *Materials Science and Engineering B*[J], 2011, 176(19): 1585
13 Baltazar Hernandez V H, Panda S K, Kuntz M L *et al*. *Materials Letters*[J], 2010, 64(2): 207
14 Sawanishi C, Ogura T, Sumi H *et al*. *Materials Science and Technology*[J], 2012, 28(12): 1459
15 Baltazar Hernandez V H, Panda S K, Okita Y *et al*. *Journal of Materials Science*[J], 2010, 45(6): 1638
16 Maie P, Pichter A, Faulkner R G *et al*. *Materials Characterization*[J], 2002, 48(6): 329
17 Lee D. *Journal of Alloys and Compounds* [J], 2009, 480(2): 347
18 Sneddon I N. *Mathematical Proceedings of the Cambridge Philosophical Society*[J], 1948, 44(4): 492
19 Hao Y L, Niinomi M, Kuroda D *et al*. *Metallurgical and Materials Transactions A*[J], 2002, 34(4): 1007
20 Hon Y H, Wang J Y, Pan Y N. *Materials Transactions*[J], 2003, 44(11): 2384
21 Kim H S, Kim W Y, Lim S H. *Scripta Materialia*[J], 2006, 54(5): 887
22 Tang F, Awane T, Hagiwara M. *Scripta Materialia*[J], 2002, 46(2): 143
23 Swadener J G, George E P, Pharr G M. *Journal of the Mechanics and Physics of Solids*[J], 2002, 50(4): 681

热变形对 TC11/Ti_2AlNb 电子束焊接件力学性能的影响

秦　春[1,2]，姚泽坤[2]

(1. 北方民族大学，宁夏 银川 750021)

(2. 西北工业大学，陕西 西安 710072)

摘　要：应用纳米压痕和维氏硬度的方法表征了 TC11/Ti_2AlNb 电子束焊接件焊缝区域在不同状态下的硬度和弹性模量分布，结合微观组织演变分析了微纳米尺度的力学变化。结果表明：在 TC11 合金的热影响区，马氏体 α'相的分解是显微硬度降低的主要原因；而在焊缝以及 Ti_2AlNb 热影响区区域，析出相导致了显微硬度的增加。通过热变形以及锻后热处理都能够提高焊接区域的弹性模量。相比较而言，焊接态的焊缝弹性模量只有 92 GPa；而在变形和热处理后，弹性模量的值达到了 130 GPa。通过拉伸实验结果分析，焊缝在变形及热处理后屈服强度得到了较大提高，这和焊缝区域硬度和弹性模量的变化趋势一致。

关键词：纳米压痕；钛合金；金属间化合物；力学性能；组织形貌

作者简介：秦 春，男，1987 年生，博士生，北方民族大学材料科学与工程学院，宁夏 银川 750021，电话：0951-20667378，E-mail：qinchun0131@163.com